Kovove Mater. 50 2012 309–318
DOI: 10.4149/km_2012_5_309

Martensite transformation bands studied in TiNi shape memory alloy by infrared and acoustic emission techniques

E. A. Pieczyska[1], H. Tobushi[2], K. Takeda[2], D. Stróż[3], Z. Ranachowski[1], K. Kulasiński[1], S. Kúdela Jr.[4]*, J. Luckner[1]

[1] *Institute of Fundamental Technological Research, PAS, Pawińskiego 5B, 02-106 Warsaw, Poland*
[2] *Aichi Institute of Technology, 1247 Yachigusa, Yakusa-cho, Toyota, 470-0392, Japan*
[3] *University of Silesia in Katowice, Bankowa 12, 40-007 Katowice, Poland*
[4] *Institute of Materials and Machine Mechanics, Slovak Academy of Sciences, Račianska 75, 831 02 Bratislava, Slovak Republic*

Received 19 January 2012, received in revised form 27 July 2012, accepted 13 August 2012

Abstract

TiNi shape memory alloy (SMA) specimens have been subjected to tension carried out at various strain rates. The goal was to investigate a nucleation and development of the stress-induced martensitic transformation by infrared (IR) and acoustic emission (AE) techniques. Therefore, both the infrared radiation and acoustic emission data were recorded using a fast infrared camera and acoustic emission set-up, respectively. It has been shown that the initial, macroscopically homogeneous transformation initiates in the elastic stage of the deformation even before the stress-strain curve knee and formation of the localized transformation bands. It has also been found that the homogeneous transformation occurs at similar stress level for all strain rates applied, while the localized martensitic transformation depends on the strain rate. Nucleation and development of the localized transformation bands, detected by the infrared camera, were confirmed by acoustic emission technique. The differences between the IR and AE activities were recorded during the TiNi SMA loading and unloading process, manifesting different dynamics of the stress-induced martensitic forward and reverse transformation.

K e y w o r d s: shape memory alloy, TiNi, superelasticity, martensitic transformation, tension test, acoustic emission

1. Introduction

Shape memory properties, good biocompatibility, high strength and corrosion resistance of TiNi shape memory alloys enable them to find numerous applications in automotive, aircraft, space, biomedical and also in mass consumer's goods production [1–5]. The SMA functional properties are derived from reversible martensitic transformation that occurs in solid state [3–10]. In some experimental conditions, the stress-induced martensitic transformation (SIMT) can develop in the form of Lüders-like transformation bands [7]. The transformation bands cause the alloy inhomogeneity, which can be unfavorable, especially for the biomedical applications [3]. The influence of the test conditions on the nucleation and evolution of the localized martensitic transformation have been analyzed for TiNi SMA in [3–16]. The topic is important, since due to good biocompatibility, elements of TiNi SMA are used as cardio-surgical stents, guidewires and implants. The investigation on the stress-induced transformation bands at present is carried out in different research centers, where various experimental techniques are used, e.g. the digital image correlation strain map (DIC) [4, 10], the infrared technique (IR) or the CCD camera [5–16]. As for the results presented in this paper, fast and sensitive infrared camera was used, enabling recording the temperature changes on the specimen surface with a proper frequency and sensitivity, to reflect nucleation and development of the transformation process, especially the transformation bands almost at the very time of their creation.

*Corresponding author: tel.: (+421) 2 49268 292; fax: (+421) 2 49268 312; e-mail address: ummskudm@savba.sk

An acoustic emission (AE) technique was also used in this approach to detect the propagation of related stress wave, attributed to a different dynamics of the SIMT process.

The authors who describe the AE generated during the martensitic transition mention dislocation processes and twins formation as a cause of AE activity. AE in the form of a stress wave arises when a rapid volume change locally appears in investigated material [17–19]. Particularly this state can accompany twinning processes and new inter-grain boundaries forming around the growing martensite regions. Since due to the phase transition one can observe a sudden volumetric change in the region of forming of a martensite plate, the potential U measured in the output of AE sensor can be calculated as:

$$U = g_{33} Y_{33} D_1, \tag{1}$$

where g_{33} is piezoelectric constant of AE sensor (ca. 10^{-2} V m^{-1} N^{-1}), Y_{33} is Young's modulus of compressed AE sensor (ca. 5×10^{10} N m^{-2}), D_1 is amplitude of a stress wave caused by the volumetric change due to formation of martensite plate (m).

The collapse of martensite regions and their transition into austenitic structures are also potentially effective sources of AE activity due to volumetric changes. It was reported that monitoring of the course of martensitic transition from its start to the final stage delivers the close findings to those obtained by the measurements of the alloy resistivity.

There are a few works only published till now describing the application of acoustic emission measurements to study the development of martensitic transformation in TiNi shape memory alloy. One of the reasons is that it is still difficult to explain the acoustic emission data in terms of the fundamental understanding of the phase transformation mechanisms, however, different approaches have been published, e.g. [17–21].

In this paper, various experimental techniques were applied in order to gather more information and attain more comprehensive insight into the TiNi shape memory alloy behavior under various loading conditions. By comparison of the obtained mechanical characteristics, temperature changes and acoustic emission signals, recorded during the process of the TiNi SMA loading and unloading, a nucleation and development of the stress-induced martensitic transformation was studied.

2. Experimental details

2.1. Material and specimens

The TiNi shape memory alloy used in the experiment is characterized by a fine nanostructure of uniformly distributed regular grains of the B2 phase with the average diameter of approximately 80 nm (Fig. 1). Some dislocations can be observed inside the grains, they mainly form low-angle boundaries between crystalline blocks (Fig. 1b). The diffusion streaks visible at some diffraction patterns along <110> directions (Fig. 1b) allow us to suggest that the material is in the state close to the R-phase transformation.

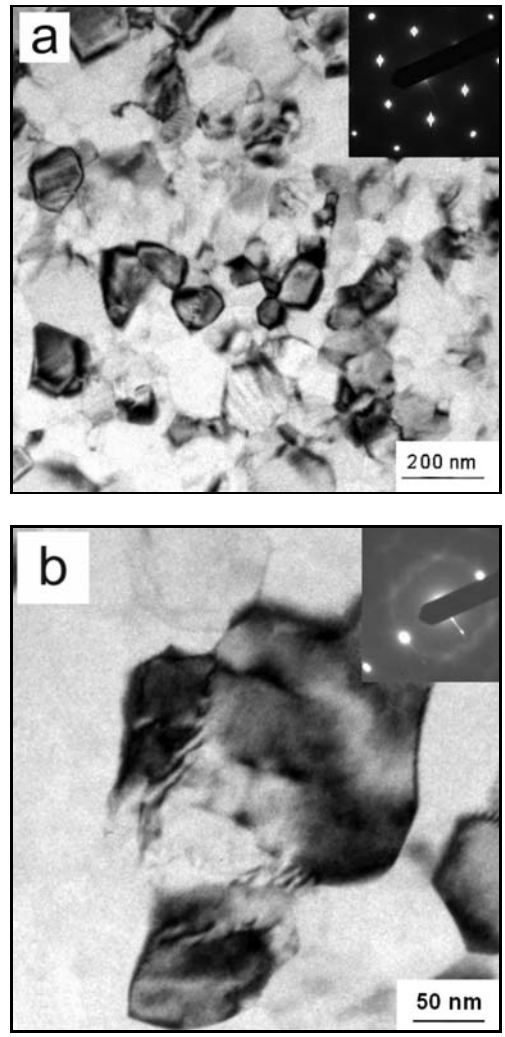

Fig. 1. Structure of TiNi SMA specimen reference state, the attached diffraction patterns prove presence of the B2 phase in the sample. a) and b) differs only by the scale; b) is zoomed in to highlight the grain structure.

Indeed, the DSC cooling curve for the alloy (Fig. 2) shows that the R-phase transition starts at $\sim$ 10 ℃. A single, wide peak is visible on this curve between –40 ℃ and +8.4 ℃. When heating, a slight bump can be noticed on the curve, which indicates possibility of overlapping of the two transformations, i.e. B19' → R → B2 or two-stage R → B2 transformation. The effect of the two-stage transformation will be discussed

a)

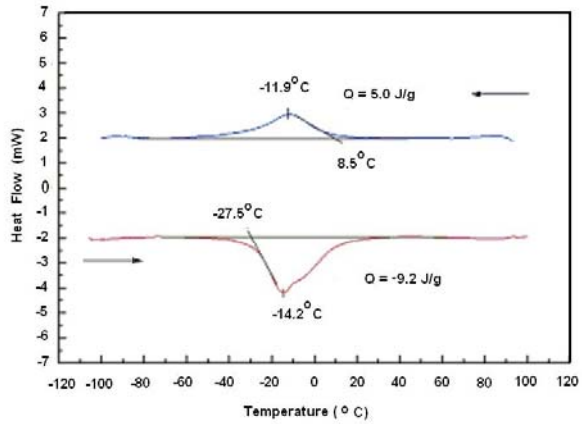

b)

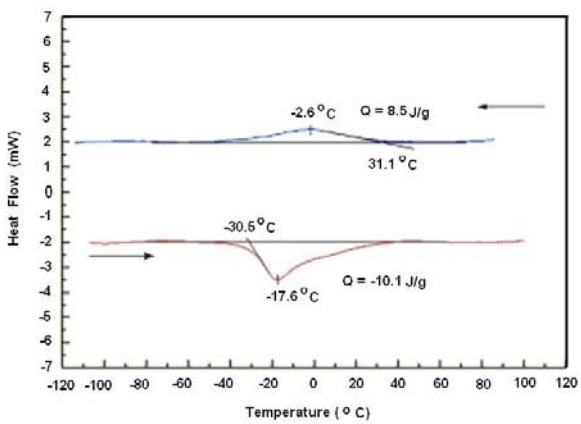

Fig. 2a,b. Differential scanning calorimetry curves for two complete heating-cooling runs of the TiNi SMA: as initial state (above), after 10 loading-unloading cycles within 8 % of strain (below).

later with the help of the time dependence of acoustic emission activity. Thermal hysteresis between the forward and reverse transformation is approximately 4 ℃. The effect of relatively greater heat production during martensite → austenite phase transformation presented in Fig. 1 corresponds to higher amount of acoustic emission energy registered during that transition, what will be reported in next paragraphs.

The TiNi SMA transformation temperatures determined by the DSC technique are as follows: R_s = 8 ℃, R_f = –36 ℃, A_s = –27 ℃, A_f = 20 ℃. Therefore, the material was superelastic at the room temperature (23 ℃) and its isothermal stress-strain curve manifested a large hysteresis loop [1]. The transformation temperatures obtained by the DSC measurements confirm the SMA chemical composition as Ti-50.5at.%Ni [2].

Also, X-ray diffraction patterns obtained for the TiNi initial state prove that the SMA at room temperature is in the B2 structure (Fig. 3). Similar result was obtained for the specimen after 20 loading--unloading cycles, which means that the reversible straining within 8 % tension range does not change the shape memory alloy phase structure.

2.2. Description of tension test

The investigation of the mechanical, thermomechanical and acoustic emission properties of the TiNi shape memory alloy was carried out on Instron testing machine. The belt type specimens of approximately 160 mm × 10 mm × 0.38 mm, cut off from the alloy strip, were subjected to tension tests carried out at various strain rates. The testing machine was controlled by a mechanical extensometer. Specially designed and made of a light polymer grip was used in

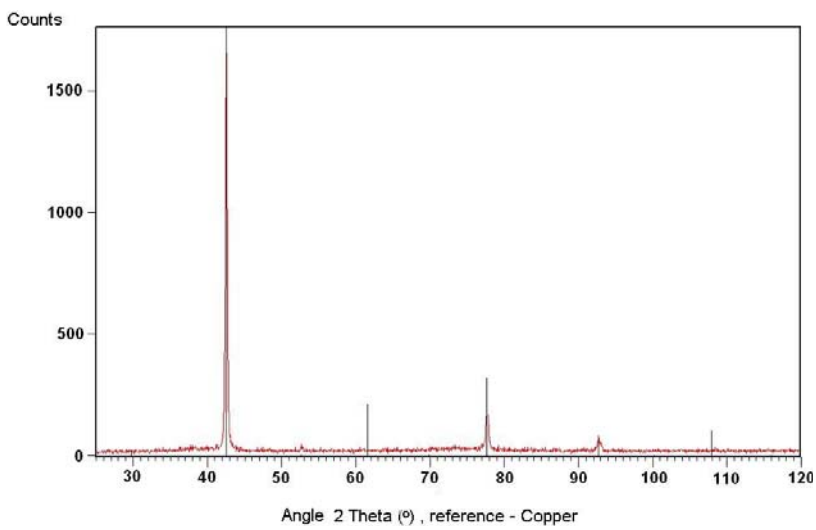

Fig. 3. X-ray diffraction pattern of the TiNi SMA initial state.

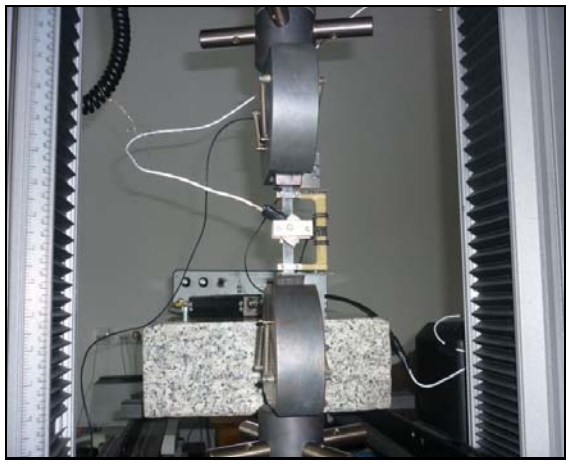

Fig. 4. TiNi SMA specimen in grips of the Instron testing machine with acoustic emission sensor placed in the central part of the specimen.

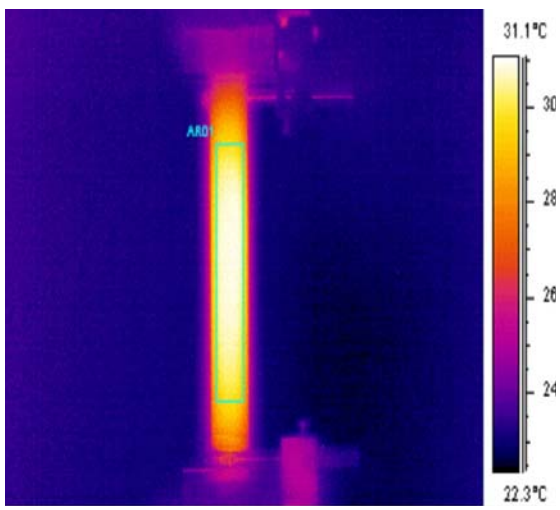

Fig. 5. The green square, visible in the specimen surface defines specimen area chosen to calculate a mean temperature measured during the transformation process.

order to fit the extensometer to these rather thin specimens (Fig. 4).

In the course of the loading, both the mechanical characteristics and the distribution of the infrared radiation emitted by the specimen surface were continuously recorded. The stress and strain quantities were related to the current values of the specimen cross-section and thickness, obtaining in this way so called true stress and true strain values, presented in the graphs. Since due to the mutual interactions it is not possible to use infrared and acoustic emission techniques at the same time, a similar loading program was applied in order to record the acoustic emission signals, accompanying the process of the stress-induced martensitic transformation.

Finally, by comparison of the obtained mechanical characteristics, temperature changes and acoustic emission signals, a nucleation and development of the stress-induced martensitic transformation was studied.

2.3. Description of the infrared technique

The changes of the specimen temperature, accompanied the exothermic martensitic forward transformation during the SMA loading and the endothermic reverse one during the unloading, were recorded using a very fast and sensitive infrared camera Phoenix, Flir Co., working in the wavelength range of 3.5–5.0 μm. Before the testing, the specimen surface was covered with very thin layer of black ink. This was made to obtain more homogeneous surface with higher and known coefficient of emissivity. The camera recorded the infrared radiation from the specimen surface and a system of the data acquisition and conversion allowed for infrared photographs, i.e. thermograms, to be stored in digital form with high frequency of 538 Hz. This enables reproduction of the images at any time, and enables calculation of the specimen average temperature from a randomly chosen specimen area, line, points, etc. with high accuracy and sensitivity, of approximately 0.025 K.

Taking into account the specimen emissivity and the specimen-camera distance, the average specimen temperature changes accompanying the martensitic transformation were calculated. The average temperature was calculated over an area of $8 \times 60\,\mathrm{mm}^2$, located in the central part of the specimen (Fig. 5). The mean specimen temperature obtained in this way can be presented as a function of strain, time or other parameters of the deformation process.

2.4. Description of the acoustic emission technique

The AE signals were recorded using a wide-band AE sensor of WD type, produced by Physical Acoustic Corporation. The sensor was fixed to the TiNi tape with application of elastic rubber band. Total amplification of the AE analyzer was 70 dB and the sampling frequency was 44.1 kilosamples per second. AE signal in digital form was stored in a hard disk. The analyzing software was prepared to create the time dependence of AE events rate per second. AE event was recognized in the source form of AE signal using the algorithm capturing the moments when the signal amplitude was exceeding the level of 10 μV. The shortest duration of the event was set to 70 μs. The aim of creating the graphs of AE activity was to apply a tool for comparison of temporal intensity of both simple and reverse martensitic transition. Standard formula enabled the authors of the paper to calculate the AE

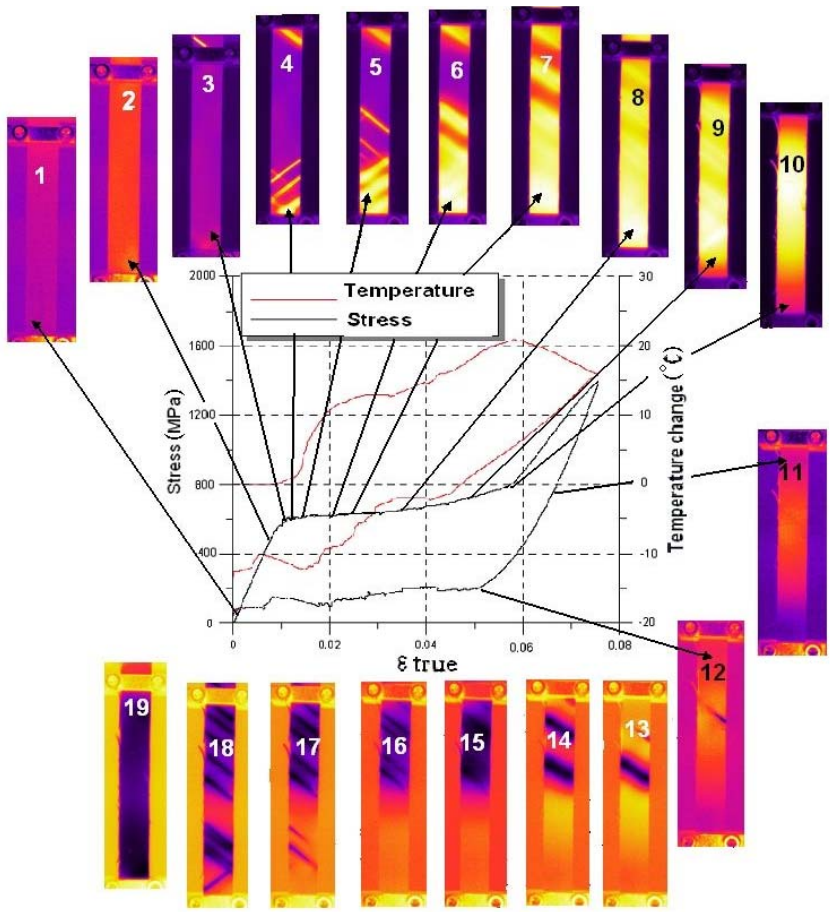

Fig. 6. Stress and temperature changes vs. strain curves obtained for TiNi SMA during tension at strain rate $10^{-3}\,s^{-1}$. Thermograms show in infrared a nucleation and evolution of macroscopic transformation bands, related to martensite forward (1–10) and reverse (11–19) transformation. Colors on thermograms scaled similar to range shown in Fig. 5.

signal energy registered during the forward and reverse martensitic transition, separately:

$$E_{\mathrm{AE}} = \frac{1}{Z}\sum_i x_i^2 \frac{1}{f}, \tag{2}$$

E_{AE} denotes the energy of acoustic emission signal (pJ), Z is the impedance of the experimental setup ($1000\,\mathrm{V\,A^{-1}}$), x_i is the voltage registered at a single sampling cycle (V), f is the system sampling frequency ($\mathrm{s^{-1}}$).

3. Results and discussion

3.1. Mechanical characteristics, infrared imaging and temperature variations

In order to assure proper conditions for all the measurement techniques applied, the adequate strain rate must be chosen: not too low and not too high. In our approach, a test with strain rate $10^{-3}\,s^{-1}$ was chosen as to present and analyze the onset and growth of the stress-induced martensitic transformation in infrared and acoustic emission techniques. Stress-strain and average temperature change vs. strain curves accompanied by infrared imaging of macroscopic transformation bands recorded for TiNi SMA subjected to complete loading and unloading tension cycle within 8 % strain range, are presented in Fig. 6. The thermograms that have been distributed around the graph show the temperature distribution on the specimen surface reflecting a nucleation and evolution of the SIMT. The uniform temperature distribution observed on the specimen surface indicates homogeneity of the stress and strain state along the specimen. Before the tension was started, the temperature of the specimen was uniform and equal to the ambient temperature (Fig. 6: 1st thermogram). At the certain level of the stress and strain state, the temperature of the specimen starts to grow slowly, however, its thermal image remains uniform, indicating the homogeneous nature of the initial phase transformation process (Fig. 6: 2nd thermogram). At higher strains, inclined bands of significantly higher temperature are observed, starting

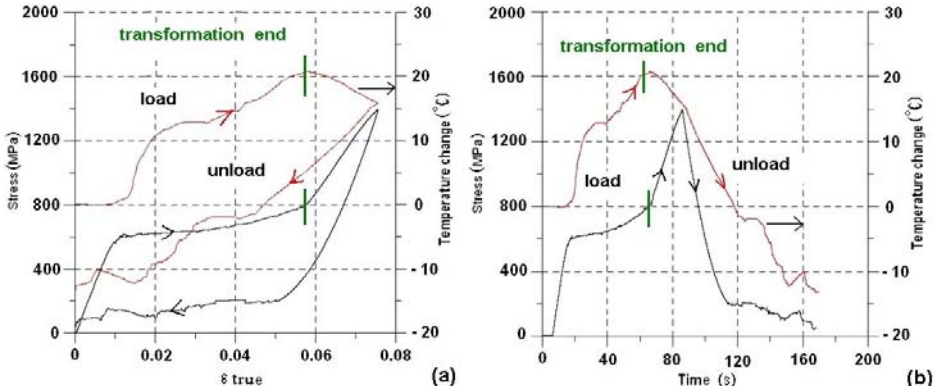

Fig. 7. Stress and temperature change vs. strain curves (a) and vs. time (b) obtained for TiNi SMA specimen during tension at strain rate 10^{-3} s^{-1}.

in the specimen grip areas and developing towards the specimen center (Fig. 6: thermograms 3–7). They were called transformation bands or Lüders-like deformation and were reported in some papers [3, 7, 9, 12]. The shape of transformation bands appeared in the same form during several repetitions made by the authors of the paper. The bands of the new martensite phase are characterized by the angle of inclination with the direction of tension of approximately 48° in this case, and the variation in temperature of approximately 8 K. The slope of the transformation bands changes slightly during the loading and transformation process, since it depends on the specimen geometry [9]. The place of the nucleation of the localized transformation depends on the specimen homogeneity, according to the alloy structure and the local stress state, caused e.g. during the mounting of the specimen in the grips of the testing machine. The initial transformation bands are followed by a next generation of the bands developing in almost perpendicular direction (Fig. 6: thermograms 4, 5). The bands gradually widen and overlap. The average specimen temperature increases very fast due to the instantaneous heat production related to the exothermic martensitic transformation, however, due to the overlapping effects its specimen thermal image becomes more uniform at this advanced transformation stage (Fig. 6: thermograms 7–9). After this very intense transformation stage, a decrease of the specimen average temperature is observed at the final part of the SMA loading process (Fig. 6: thermogram 10, and Fig. 7). The drop in temperature confirms that at this loading stage the transformation starts to be saturated. Namely, from this loading and transformation stage, the heat flow to the surrounding starts to overcome the heat production caused by the exothermic martensitic transformation. As it was confirmed by other study and microstructure analysis, it does not mean that the stress-induced transformation is fully completed, but from this stage the process is not so intense [7–13].

In the course of unloading, the specimen temperature decreases significantly (Fig. 6: thermograms 11–19, Fig. 7). The bands of significantly lower temperature are developed (Fig. 6: thermograms 12–18). The bands also develop in two directions and they are inclined by the similar slope. Finally, just after the unloading was completed, the specimen temperature drops by about –12 K, below its initial temperature (Fig. 6: thermogram 19, and Fig. 7). Similar TiNi SMA thermomechanical behavior, studied under various programs of the loading and martensitic transformation, was discussed in more details in [16].

The stress and mean temperature results obtained for the same test and presented as a function of strain (a) and time (b) are shown in Fig. 7. The initial, elastic range of the loading, characterized by high elastic modulus, is followed by the next stage, where the elastic modulus is rather low. This stage is associated with the intense transition of the parent austenite into martensite phase. The average temperature of the specimen starts to increase even before the stress--strain knee, at approximately 400 MPa, manifesting the onset of the phase transformation at this stage, since the SIMT is exothermic [5, 9, 10, 12, 13]. Especially the advanced transformation, developing in the bands that have been shown in infrared in Fig. 6, is associated with a huge heat production and the significant temperature increase, over 20 K in this case, since the recorded temperature changes depend on the strain rate applied [9, 12].

Both the stress and the average temperature presented as a function of time (Fig. 7b) show that the SMA loading and unloading processes are nonsymmetrical, i.e., the run of the recorded stress and the average temperature changes is quite different. Such a behavior is associated with the difference between the mechanisms of the stress-induced martensitic forward and reverse transformation. This is related to the significant difference between the parent austenite and the resulting martensite phase structure. During the martensitic forward transformation, in the case of TiNi SMA, the parent cubic (β) with a B2 superlat-

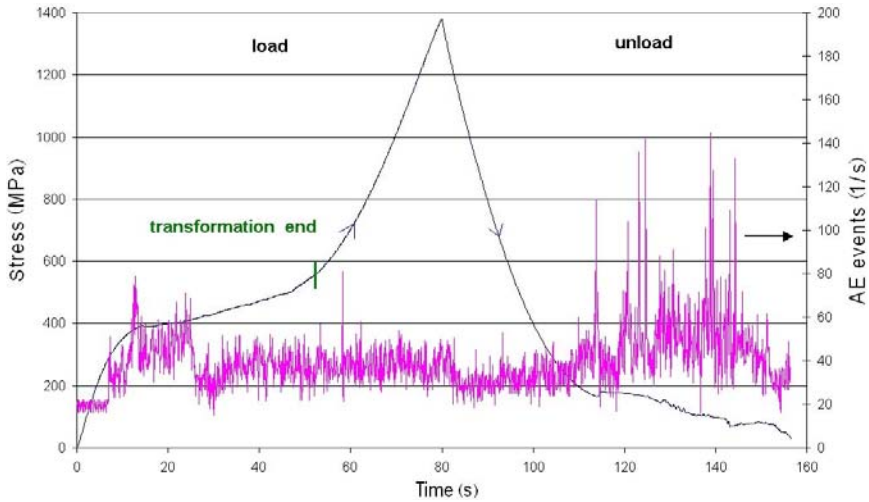

Fig. 8. Stress and acoustic emission count rates obtained for TiNi SMA pseudoelastic behavior during loading and unloading with strain rate $10^{-3}\,s^{-1}$.

tice (BCC) structure transforms into the monoclinic B19' structure. In order to form such a martensite structure, twins, dislocations or stacking faults are introduced. It was experimentally confirmed that especially transformation-induced twins played important role during the martensitic transformation in TiNi shape memory alloys [22]. On the other hand, it was found in other experiments using acoustic emission technique, that the processes of twins formation constituted strong sources of acoustic emission signals, reflecting dynamic change in the material structure. This was the reason that we decided to use the acoustic emission technique in order to obtain more information on the mechanisms of the stress-induced martensitic forward and reverse transformation in the SMA.

3.2. Mechanical characteristics and acoustic emission measurements

In order to compare the process of the SIMT, both nucleation and development studied by the infrared and acoustic emission techniques, the following results were obtained for the same TiNi SMA specimens, subjected to tension at various strain rates, while the acoustic emission signals from the specimens were measured. The obtained results of the stress and AE count rates, recorded for the martensitic forward and reverse transformation, during the SMA loading and unloading, respectively, are presented in Figs. 8–12.

The stress and the acoustic emission count rate results recorded during the TiNi SMA superelastic tension with the strain rate $10^{-3}\,s^{-1}$, the same as presented in Figs. 6 and 7, are shown in Fig. 8. The onset of the AE signal during the SMA loading is rapid and appears before the knee of the stress-strain curve. Such an acoustic emission behavior confirms the nucleation of the initial homogeneous martensitic transformation, manifested by the beginning of the temperature increase in Fig. 6: thermogram 2 and in Fig. 7a,b. Some significant acoustic emission signals were also observed for the subsequent, localized transformation, especially at the stage while the localized transformation bands are created, reflecting by waving part of the stress-strain characteristics. In the meantime, not so significant AE signals were recorded at the stage of the advanced transformation, being the final one of the SMA loading. It confirms that the strong AE signals are created by a sudden change in the material or process state, not by the same process, even if the process develops very fast [17–21]. Moreover, looking at Fig. 8, one can observe that the AE signals recorded during the SMA unloading for the martensitic reverse transformation, are much stronger in comparison to the forward transformation, observed during the SMA loading. Particularly strong signals were recorded at the final stage of the specimen unloading, reflecting the last part of the reverse transformation. It means that the reverse transformation, targeted on the returning of the specimen to the initial shape and the austenite parent phase structure reveals in other manner in comparison to the forward austenite-martensite transition.

The initial homogeneous stage of the martensitic forward transformation was also confirmed by the acoustic emission measurements performed on the TiNi SMA at the lower strain rate equal to $10^{-4}\,s^{-1}$ and presented in Fig. 9.

For so low strain rate, the test conditions are close to an isothermal one. As it was found in our former tests, for this strain rate the recorded temperature changes are about 4 K [12]. Therefore, the SMA flow, related to the SIMT, starts on the stress level of approximately 480 MPa and is keeping almost constant

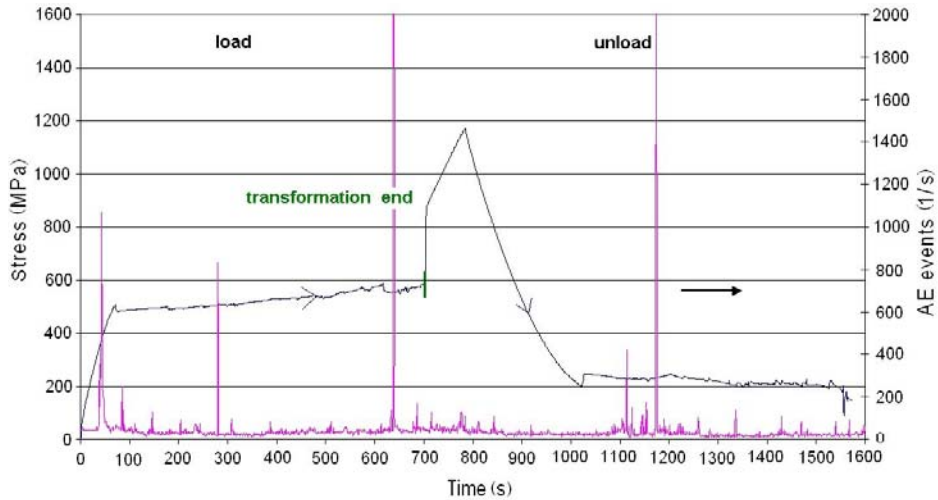

Fig. 9. Stress and acoustic emission count rates obtained for TiNi SMA pseudoelastic behavior during loading and unloading with strain rate $10^{-4}\,s^{-1}$.

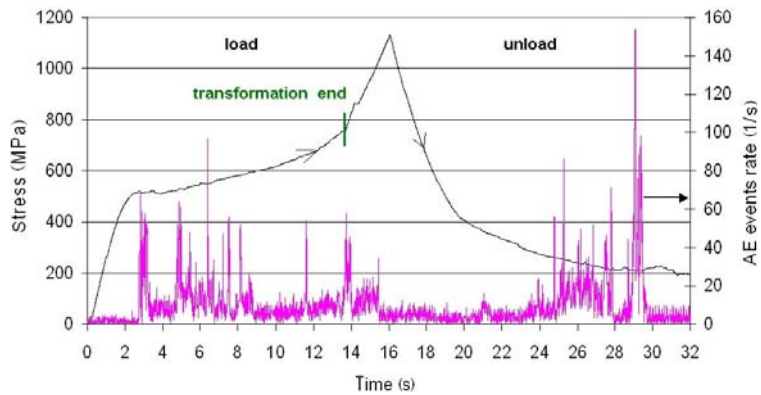

Fig. 10. Stress and acoustic emission count rates obtained for TiNi SMA pseudoelastic behavior during loading and unloading with strain rate $5 \times 10^{-3}\,s^{-1}$; test 1.

during the loading, developing till only 580 MPa. However, even for so low strain rate, some significant AE signals were recorded, the first at the stress of approximately 400 MPa, as it was observed by the temperature changes and acoustic emission signals for the strain rate $10^{-3}\,s^{-1}$. The oscillations which can be noticed on the stress-time curve are associated with the creation of the localized transformation bands.

3.3. Stress-induced martensitic transformation in TiNi shape memory alloy. Assessment of acoustic emission measurements repeatability and acoustic emission energy

The goal of the next step of the experiment was to examine how far the process of the mechanical characteristics and their related acoustic emission measurements, was repeatable. For this purpose a strain rate of $5 \times 10^{-3}\,s^{-1}$ was chosen and three subsequent loading-unloading tests were performed, each time on the new TiNi SMA specimens, within the strain range of 8 %, i.e. the same as it was used in the all former tests. The obtained results are presented in Figs. 10–12, respectively. The strain rate $5 \times 10^{-3}\,s^{-1}$ was five times higher in comparison to those presented in infrared in Figs. 6 and 7, and by AE measurements in Fig. 8. The latent heat that is released during the loading and transformation process in these conditions raises the specimen temperature up to 30 K [12], which follows the increase of the stress value required to develop the transformation, from approximately 520 MPa till about 800 MPa (Figs. 10–12). After the latter level (ca. 800 MPa) is exceeded the elastic phase of martensite deformation appears.

It can be noticed from the figures that acoustic emission signals of minor intensity were recorded at the end of the elastic part of the stress-strain curve, before the stress knee, as it was recorded in the former tests for lower strain rates (Figs. 8 and 9). Probably, the strain rate $5 \times 10^{-3}\,s^{-1}$ is so fast that due to the inertia effects there is not enough time to record the

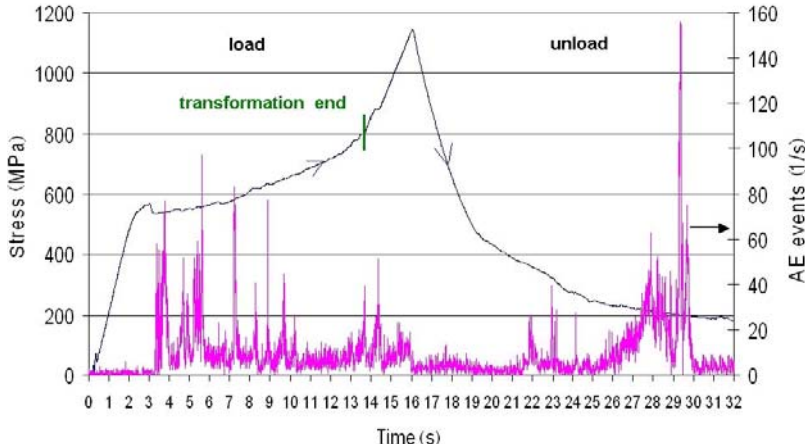

Fig. 11. Stress and acoustic emission count rates obtained for TiNi SMA pseudoelastic behavior during loading and unloading with strain rate 5×10^{-3} s^{-1}; test 2.

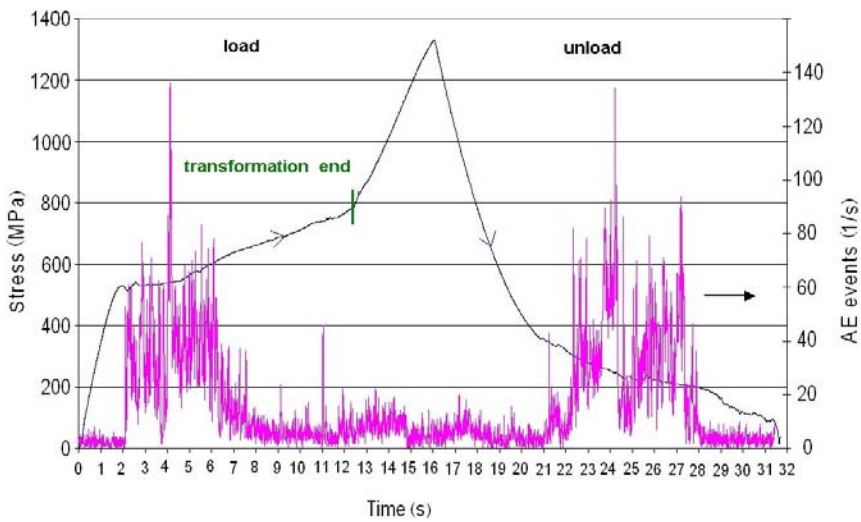

Fig. 12. Stress and acoustic emission count rates obtained for TiNi SMA pseudoelastic behavior during loading and unloading with strain rate 5×10^{-3} s^{-1}; test 3.

Table 1. Comparison of the energy of AE signal recorded during three tests of TiNi SMA loading and unloading performed at strain rate 5×10^{-3} s^{-1}

Test number	AE signal energy calculated for the TiNi SMA martensitic forward transformation (pJ)	AE signal energy calculated for the TiNi SMA martensitic reverse transformation (pJ)
1	26.7	20.1
2	29.8	70.5
3	72.9	80.3

AE signals at this very short and fast elastic deformation stage.

However, just after the stress knee, significant AE signals are recorded due to the intense development of the SIMT localized transformation. Just as it was found in the former test (Fig. 8), the AE signals are much weaker at the advanced stage of the martensitic forward transformation and at the beginning of the unloading stage, when the reverse transformation starts. Nevertheless, very intense EA count rate signals were recorded at the final part of the unloading and advanced reverse transformation.

According to the repeatability of the recorded stress and the acoustic emission count rates, a discrepancy of the results shown in Figs. 10–12 is noticed. However, since many factors on the way: material phe-

nomena – AE counts rate, can influence the obtained results, the repeatability is acceptable.

During the repeated loading and unloading of the three subsequent TiNi SMA specimens, stress and AE signals were recorded and its energy related to the martensitic forward and reverse transformation was calculated, respectively. The obtained results are presented in Table 1.

Even though the results reflect a significant discrepancy due to low level of the registered signals, one can assume that the AE signal energy of the reverse martensitic transformation overcomes the amount registered during the forward run, probably because of the more complicated and longer lasting returning of the SMA to its former shape and structure.

4. Concluding remarks

The process of nucleation and development of the stress-induced martensitic transformation in TiNi shape memory alloy was studied by a fast sensitive infrared camera and acoustic emission techniques. Both the infrared and acoustic emission techniques confirm the initial, macroscopically homogeneous transformation, nucleating even before the knee of the stress--strain curve, especially for the lower strain rates. At the higher strains, the infrared camera enables us to record the formation of the localized transformation. Nucleation and development of the transformation bands, detected by the infrared camera, were confirmed by acoustic emission technique. At higher strain rates, a higher specimen temperature due to the exothermic martensitic forward transformation was obtained, which follows the higher stress, necessary for nucleation of the martensitic transformation. The differences between the AE activities, observed during the TiNi SMA loading and unloading process, have manifested different dynamics of the stress-induced martensitic forward and reverse transformation.

Acknowledgements

The research has been carried out with support of the Polish Ministry of Science and Higher Education under Grant No 501220837, the Polish National Center of Science under Grant No 2011/01/M/ST8/07754 and the Japan Society for the Promotion of Science (JSPS). The infrared measurements were performed with the contribution of M. Maj and the diagrams were elaborated by R. Maciak, to whom the authors wish to express their gratitude.

References

[1] Shaw, J. A., Kyriakides, S.: Acta Mater., *45*, 1997, p. 683. doi:10.1016/S1359-6454(96)00189-9
[2] Tang, W., Sundman, B., Sandström, R., Qiu, C.: Acta Mater., *47*, 1999, p. 3457.
[3] Sun, Q. P., Li, Z. O.: Int. J. Solids and Structures, *39*, 2002, p. 3797. doi:10.1016/S0020-7683(02)00182-8
[4] Murasawa, G., Koushinbou, M., Yoneyama, S., Sakuma, T., Takashi, M.: J. Soc. Mat. Sci. (Japan), *53*, 2004, p. 999.
[5] Brinson, L. C., Schmidt, L., Lammering, R.: J. Mech. Phys. Solids, *52*, 2004, p. 1549. doi:10.1016/j.jmps.2004.01.001
[6] Pieczyska, E. A., Gadaj, S. P., Nowacki, W. K., Tobushi, H.: Bull. Pol. Ac. Tech., *52*, 2004, p. 165.
[7] Tan, G., Liu, Y., Sittner, P., Saunders, M.: Scripta Materialia, *50*, 2004, p. 193. doi:10.1016/j.scriptamat.2003.09.018
[8] Sittner, P., Liu, Y., Novak, V.: J. Mech. Physics, *53*, 2005, p. 1719. doi:10.1016/j.jmps.2005.03.005
[9] Pieczyska, E. A., Gadaj, S. P., Nowacki, W. K., Tobushi, H.: Experimental Mechanics, Springer, *46*, 2006, p. 531. doi:10.1007/s11340-006-8351-y
[10] Daly, S., Ravichandran, G., Bhattacharya, K.: Acta Mater., *55*, 2007, p. 3593. doi:10.1016/j.actamat.2007.02.011
[11] Dutkiewicz, J. M., Maziarz, W., Czeppe, T., Lityńska, L., Nowacki, W. K., Gadaj, S. P., Luckner, J., Pieczyska, E. A.: European Phys. J. Special Topics, *158*, 2008, p. 59. doi:10.1140/epjst/e2008-00654-6
[12] Pieczyska, E. A: Prace IPPT/IFTR Reports, ISBN 978-83-89687-37-1, *3*, 2008. [Habilitation Thesis] (in Polish, graphs in English).
[13] Favier, D., Louche, H., Schlosser, P., Orgeas, L., Vacher, P., Debove, L.: Acta Materialia, *55*, 2007, p. 5310. doi:10.1016/j.actamat.2007.05.027
[14] Tobushi, H., Pieczyska, E. A., Ejiri, Y., Sakuragi, T.: Mechanics of Advanced Materials and Structures, *16*, 2009, p. 236. doi:10.1080/15376490902746954
[15] Zhang, X., Feng, P., He, Y., Yu, T., Sun, Q.: Int. J. Mechanical Sciences, *52*, 2010, p. 1660. doi:10.1016/j.ijmecsci.2010.08.007
[16] Pieczyska, E. A.: J. of Modern Optics, *57*, 2010, p. 1700. doi:10.1080/09500341003725748
[17] Speich, G. R., Fisher, R. M.: Acoustic Emission during Martensite Formation, Acoustic Emission. ASTM STP 505, American Soc. for Testing and Materials 1972, p. 140.
[18] Vacher, P., Lexcellent, C.: In: Kyoto Conf. Proceedings, 1991, p. 231.
[19] Straka, L., Novak, V., Landa, M., Heczko, O.: Mater. Sc. Eng., A, *374*, 2005, p. 263.
[20] Novak, V., Landa, M., Sittner, P.: In: Proc. of SMST'99, First European Conference on Shape Memory and Superelastic Technologies. Antwerp, Belgium 1999, p. 1.
[21] Lucia, A., Santulli, C.: J. Phys. IV France, *7*, 1997, Colloque C5, Suppl. J. de Physique, p. 637.
[22] Yamauchi, K., Ohkata, I., Tsuchya, K., Miyazaki, S. (Eds.): Shape Memory and Superelastic Alloys. Woodhead Publishing Limited 2011.